Improvement of quantum efficiency in green light-emitting diodes with pre-TMIn flow treatment

2011 J. Phys. D: Appl. Phys. 44 224015

(http://iopscience.iop.org/0022-3727/44/22/224015)

J. Phys. D: Appl. Phys. **44** (2011) 224015 (6pp) doi:10.1088/0022-3727/44/22/224015

Improvement of quantum efficiency in green light-emitting diodes with pre-TMIn flow treatment

Ya-Ju Lee[1], Yi-Ching Chen[1] and Tien-Chang Lu[2]

[1] Institute of Electro-Optical Science and Technology, National Taiwan Normal University, 88, Sec.4, Ting-Chou Road, Taipei 116, Taiwan
[2] Department of Photonics, National Chiao Tung University, 1001 Ta Hsueh Road, Hsinchu, Taiwan

E-mail: yajulee@ntnu.edu.tw

Received 29 November 2010, in final form 28 January 2011
Published 13 May 2011
Online at stacks.iop.org/JPhysD/44/224015

Abstract
The effects of pre-trimethlyindium (TMIn) flow on the improved electrical characteristics and highly stable temperature properties of InGaN green light-emitting diodes (LEDs) are discussed. For the LED sample with a pre-TMIn flow treatment, the tunnelling of injected carriers associated with threading defects is significantly reduced, which promotes the diffusion–recombination of injected carriers, as well as the overall emission efficiency of the LED. In addition, the pre-TMIn flow treatment evidently reduces the dependence of external quantum efficiency on temperature and efficiency droop of green LEDs. As a result, we conclude that the pre-TMIn flow treatment is a promising scheme for the improvement of output performance of InGaN-based green LEDs.

(Some figures in this article are in colour only in the electronic version)

1. Introduction

Light-emitting diodes (LEDs) have attracted considerable interest as candidates for next-generation lighting because they promise to reduce energy consumption enormously. LEDs directly convert electrical energy into light, and over the years their efficiency has rapidly increased to become comparable to that of fluorescent lamps [1]. In particular, the development of InGaN alloys is of primary concern in the production of LEDs that are highly efficient right across the visible spectrum. The state-of-the-art InGaN-based high-power blue LEDs can deliver an external quantum efficiency (EQE) as high as 56% [2]. Yet, the peak EQE of green LEDs is significantly lower than that of InGaN-based blue and AlGaInP-based red LEDs, which is characteristically called the 'green gap' [3]. Additionally, the efficiency of green LEDs falls more rapidly than that of blue LEDs as the injected current increases [4, 5]. Therefore, to harness the full potential of LEDs for next-generation lighting, further increases in the quantum efficiency of InGaN-based green LEDs are required. Generally, to engineer a narrow bandgap suited to emission wavelengths from $\lambda = 500$ nm to $\lambda = 570$ nm, high indium compositions of up to 30% in the quantum wells (QWs) of LEDs are essential. Such high indium compositions are associated with a complex array of properties, which can adversely affect the crystalline quality and output performance of LEDs [6]. To overcome these issues, a few studies have considered improving the optical properties and the interface abruptness of InGaN-based green LEDs by supplying a flow of trimethlyindium (TMIn) prior to the growth of the QWs [7–9]. Nevertheless, the influences of such pre-TMIn flow treatment on the output performance of LEDs have rarely been discussed. In this paper, the experimental results on the improved performance and highly stable temperature characteristics of an InGaN green LED with a pre-TMIn flow treatment are presented. In the proposed scheme, several essential properties of the LED, including the electrical characteristics and the efficiency droop, are significantly improved. The potential physical causes of the improved performance are also discussed.

2. Experiments

Figure 1(*a*) schematically depicts the green LED structure. The green LED was grown on *c*-plane (0 0 0 1) sapphire

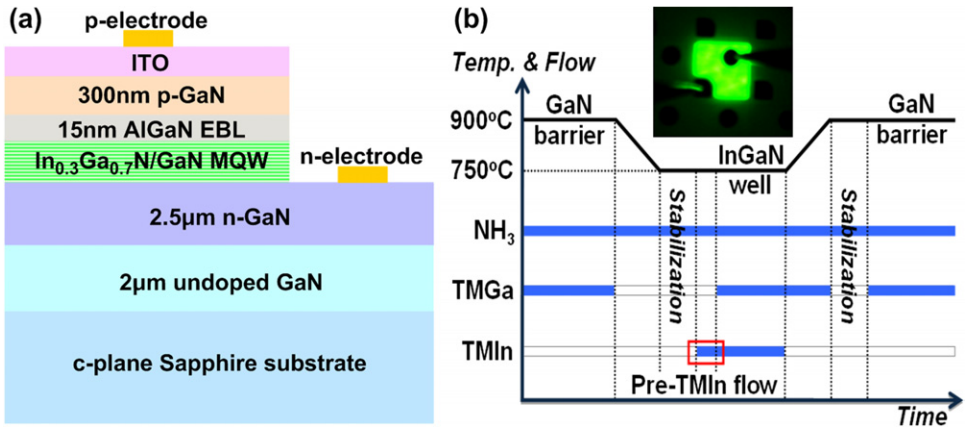

Figure 1. (*a*) Schematics of the InGaN-based green LED with pre-TMIn flow treatment during the MQWs' growth. (*b*) Time chart of the reactant sources in MQWs' growth. Inset: photograph of the green LED with pre-TMIn flow treatment taken at $I = 20$ mA.

substrates by low-pressure metal-organic chemical vapour deposition. Following the growth of a GaN nucleation layer at 520 °C, a 2 μm-thick undoped GaN layer and a 2.5 μm-thick Si-doped n-type (5×10^{18} cm^{-3}) GaN cladding layer were grown at 1050 °C. The active region composed of six periods of a nominally undoped 3 nm-thick $In_{0.3}GaN_{0.7}N$/14 nm-thick GaN multiple quantum wells (MQWs) was grown at 750 °C. The growth temperatures for the InGaN well and GaN barrier were 750 °C and 900 °C, respectively. Figure 1(*b*) plots the time chart of the reactant sources for the growth of MQWs. An interruption between the growths of well and barrier layers was used to stabilize the reactor temperature and gas flows, as shown in figure 1(*b*). During the interruption of growth, a TMIn flow of 60 sccm was introduced into the reactor prior to the growth of an InGaN well for 10 s. Furthermore, during the growth temperature ramping (from 750 °C to 900 °C), a 2 nm-thick GaN capping layer was grown on the well layer to prevent the decomposition of the InGaN well layer. Finally, a 15 nm-thick Mg-doped (1×10^{18} cm^{-3}) $Al_{0.15}Ga_{0.85}N$ electron-blocking layer (EBL) and a 300 nm-thick p-type (1×10^{18} cm^{-3}) GaN cladding layer were grown on top of the QWs. The grown wafer was then fabricated into LED chips with a mesa size of $300 \times 300\,\mu$m^2 by a standard photolithographic process, which were used for subsequent measurements. A 200 nm-thick indium tin oxide layer was deposited as a current spreading layer and Cr/Au was then deposited as n and p electrodes. The photograph of the green LED with the pre-TMIn flow treatment taken at $I = 20$ mA is shown in the inset of figure 6(*b*). For comparison, a control LED sample obtained by not introducing the TMIn flow prior to the well layers was also grown and fabricated. In this study, the optical properties of the green LED were measured using a TRIAX 190 spectrometer. The LED sample was mounted on the copper block of a cold cryostat to vary the ambient temperature over the range 77–400 K. The LED sample was biased using a ILX LDP-3811 pulsed current source with a pulse width of 6.5 μs and a duty cycle of 0.1%.

3. Results and discussion

Figure 2 shows the cross-sectional transmission electron microscopic (TEM) images of the MQWs for LED samples (*a*) without and (*b*) with pre-TMIn flow treatment, respectively. The boundaries of the InGaN/GaN QWs in both samples are clear and well defined, suggesting that the pre-TMIn flow treatment slightly affects interface abruptness. Figures 2(*c*) and (*d*) present the high-resolution TEM images of the LED samples without and with pre-TMIn flow treatment, respectively. Clearly, indium atoms are segregated along the (0 0 0 1) growth direction in both samples (blurred dark stripe), suggesting that the desorption of indium and its subsequent penetration into the GaN barrier layer remain in the sample that underwent the pre-TMIn flow treatment. Figure 3 plots the atomic force microscopy (AFM) images of the LED samples (*a*) without and (*b*) with pre-TMIn flow treatment, respectively. Both LED samples were etched with phosphoric acid to form etch pits on their surfaces [10]. The densities of etch pit estimated from figures 3(*a*) and (*b*) were 5.7×10^9 cm^2 and 7.5×10^9 cm^2, respectively. The slightly higher density of the threading dislocation in the sample that underwent the pre-TMIn flow treatment could be due to its higher indium content in the QW compared with the conventional LED.

Next, we discuss the temperature dependence of the electrical characteristics of the LED samples. Figure 4 displays the forward-bias I–V curves on a semi-log scale of the LED samples (*a*) without and (*b*) with pre-TMIn flow treatment for temperatures ranging from 77 to 400 K. Generally, the I–V curves of both samples at all temperatures exhibit the typical current rectification of InGaN-based LEDs. As shown in figures 4(*a*) and (*b*), I_Ps of both LED samples are insensitive to temperature and have similar values ($I_P \sim 10^{-11}$ A). This can be attributed to the fact that the leakage paths of the injected carriers that bypass the junction region of the LED are barely changed or influenced by varying the ambient temperature of the LEDs. More importantly, almost equal values of I_P for both LED samples suggest that the fabrication of LEDs is stable and reproducible. To further examine the I–V characteristics of

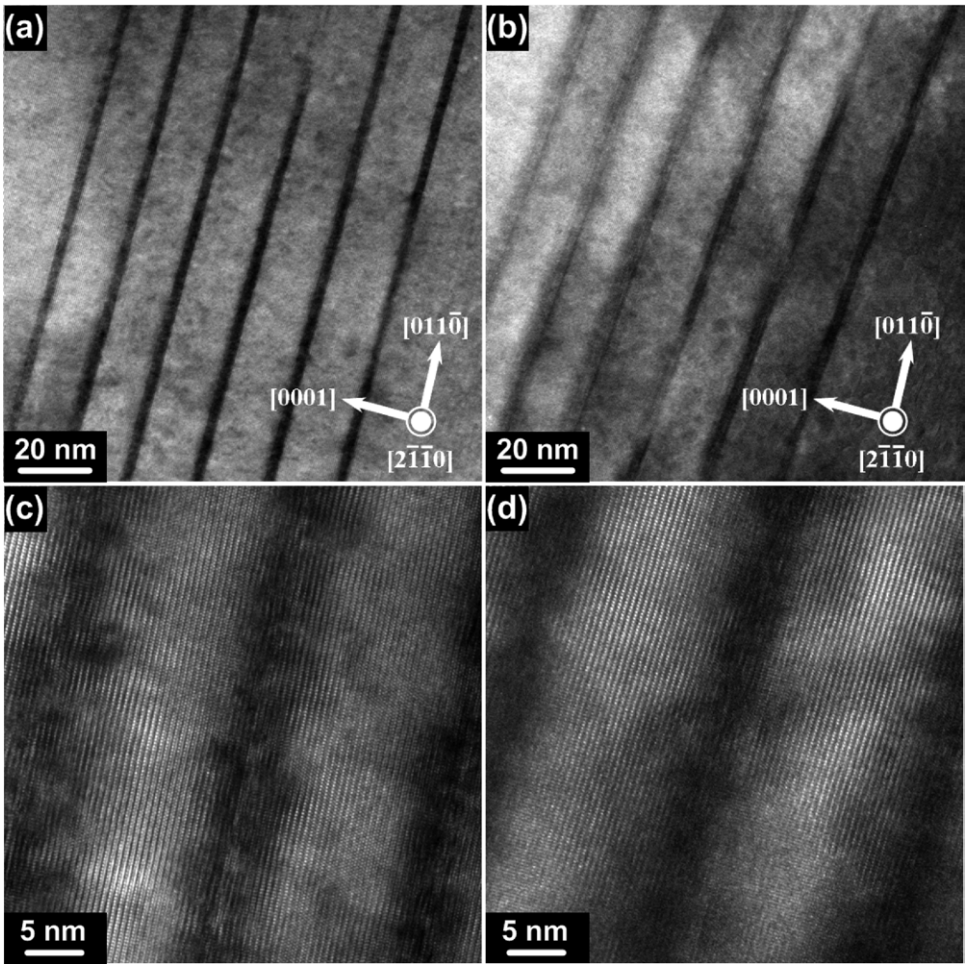

Figure 2. Bright-field TEM images of InGaN/GaN MQWs grown (*a*) without and (*b*) with pre-TMIn flow treatment. Enlarged TEM images of samples (*c*) without and (*d*) with pre-TMIn flow treatment.

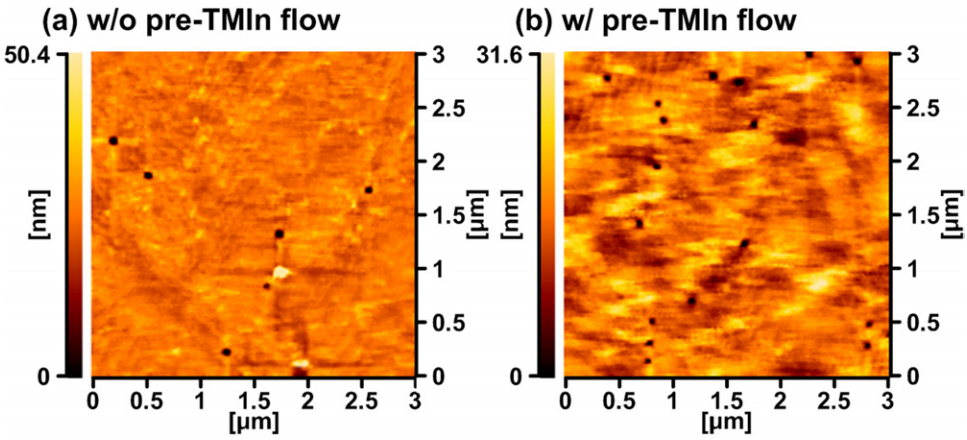

Figure 3. AFM images of the surfaces of LED samples prepared (*a*) without and (*b*) with pre-TMIn flow treatment.

the samples, the turn-on voltage (V_{on}) and the series resistance (R_S) of both samples for all temperatures are extracted and presented in figure 4(*c*). Clearly, the values of V_{on} and R_S for both samples slowly decline as the temperature increases. V_{on} of both samples decreases from 4.5 V at 77 K to 2.5 V at 400 K, mainly because of a shrinkage of the energy bandgap of (In)GaN material as the temperature increases, reducing the magnitude of the potential barrier for injected carriers to surpass and prompting the injected carriers to flow into the active region at elevated temperatures [11]. Similarly, R_S of both samples decreases from 32 to 15 Ω with the same change in temperature, mainly because of the improvement in the p-type transport properties as the temperature increases, promoting the activation of acceptors at elevated temperatures.

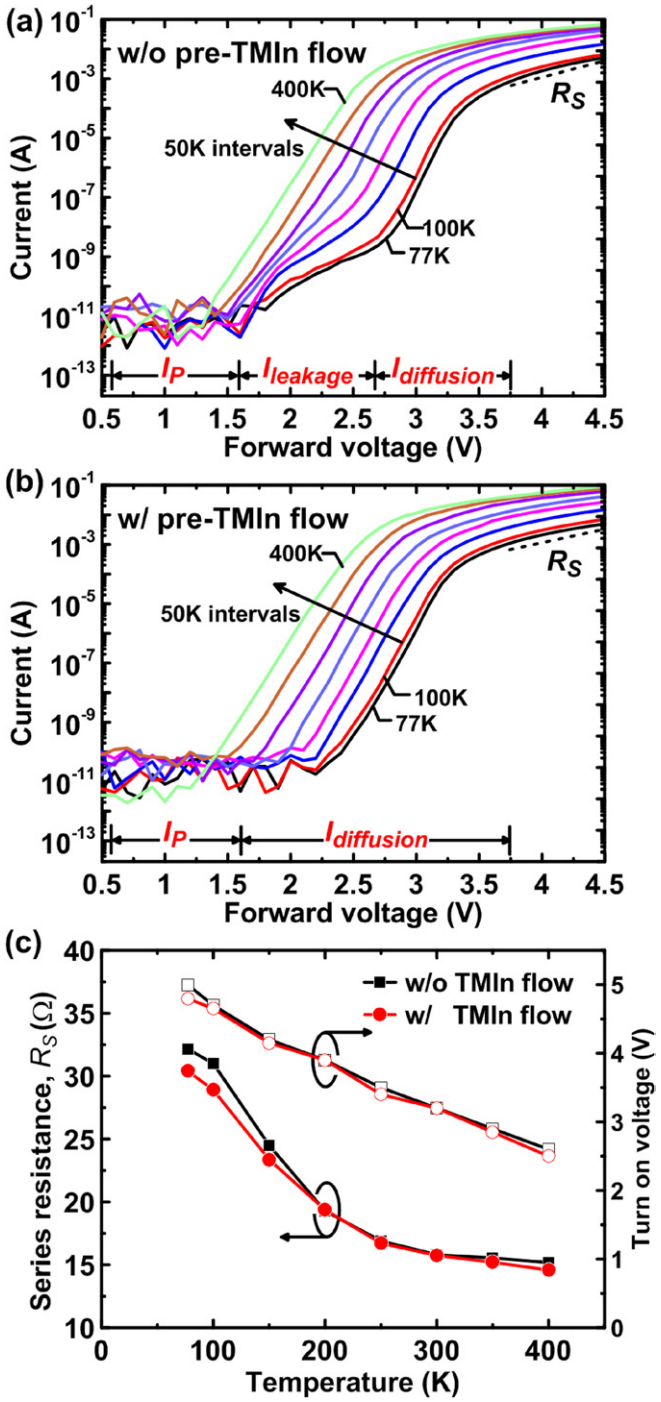

Figure 4. ln |*I*| versus *V* for the sample (*a*) without and (*b*) with pre-TMIn flow treatment from $T = 77$ K to $T = 400$ K. (*c*) Turn-on voltage (V_{on}) and series resistance (R_S) versus temperature for both LED samples.

Moreover, as shown in figure 4(*c*), at a given temperature, the values of V_{on} and R_S for both samples are similar, suggesting that the pre-TMIn flow treatment barely affected the transport property of injected carriers under forward bias injection.

In general, the *I*–*V* curve of the InGaN-based LED is well described by the Shockley equation, which takes into account the defect-assisted leakage and diffusion–recombination currents, as well as the parasitic effect [12–15]. Accordingly, the total injected current of LEDs, *I*, is given by

$$I = I_P + I_J = I_P + I_{leakage} + I_{diffusion}, \quad (1)$$

where I_P represents the current that bypasses the junction region and is given by $I_P = (V - IR_S)/R_P$, and R_P denotes the parallel resistance of the LED. I_J is the current that flows across the junction, and comprises the defect-assisted leakage current, $I_{leakage}$, and the diffusion–recombination current, $I_{diffusion}$. Both $I_{diffusion}$ and $I_{leakage}$ are given by

$$I_{leakage} = I_{O1}\left(\exp\left(\frac{e(V - IR_S)}{n_1 kT}\right) - 1\right), \quad (2)$$

$$I_{diffusion} = I_{O2}\left(\exp\left(\frac{e(V - IR_S)}{n_2 kT}\right) - 1\right), \quad (3)$$

where I_{O1} and I_{O2} are saturation currents produced by the defect-assisted leakage and the diffusion–recombination processes, respectively, n_1 and n_2 are the ideality factors for the defect-assisted leakage and the diffusion–recombination processes, respectively. Substituting equations (2) and (3) into equation (1) and considering $I_P = (V - IR_S)/R_P$, the *I*–*V* curve of an InGaN LED can be rewritten as

$$I = \frac{(V - IR_S)}{R_P} + I_{O1}\left(\exp\left(\frac{e(V - IR_S)}{n_1 kT}\right) - 1\right) + I_{O2}\left(\exp\left(\frac{e(V - IR_S)}{n_2 kT}\right) - 1\right). \quad (4)$$

As compared with the *I*–*V* curve of the LED with pre-TMIn flow treatment shown in figure 4(*b*), an obvious defect-assisted leakage process is observed in the LED without the pre-TMIn flow treatment from $T = 77$ K to $T = 250$ K (figure 4(*a*)). Such a defect-assisted leakage process becomes less significant as the temperature is further increased to 400 K. In contrast, no defect-assisted leakage process is observed in the LED with the pre-TMIn flow treatment at any temperature. Researchers have reported that indium atoms can preferentially bond at the core of a threading dislocation, pinning it, and thus preventing gliding during growth [16]. Therefore, when pre-TMIn flow is supplied, the tunnelling of injected carriers that are associated with threading defects is significantly reduced, prohibiting the recombination of injected carriers via the defect-assisted leakage process. As a result, for the LED with the pre-TMIn flow treatment, it is mainly the diffusion–recombination current that flows through the depletion region and dominates the LED. Notably, although the *I*–*V* characteristics of both LED samples at and above room temperature are very similar, the influence of threading defects on the sample that underwent the pre-TMIn flow treatment is reduced, hence improving its internal quantum efficiency, which leads to a higher light output power compared with the conventional LED.

We theoretically fitted the *I*–*V* curves plotted in figures 4(*a*) and (*b*) to obtain the saturation currents (I_{O1} and I_{O2}) of both LED samples using equation (4), where the ideality factor and series resistance of both LED samples were determined using $n_{ideal} = (q/kT)(\partial \ln I/\partial V)^{-1}$ [17] and $R_S = \partial V/\partial I$, respectively. In addition, the parallel resistances of both LED samples are set to be constants ($R_P \sim 150$ GΩ) for all temperatures, because I_Ps of both LED samples are

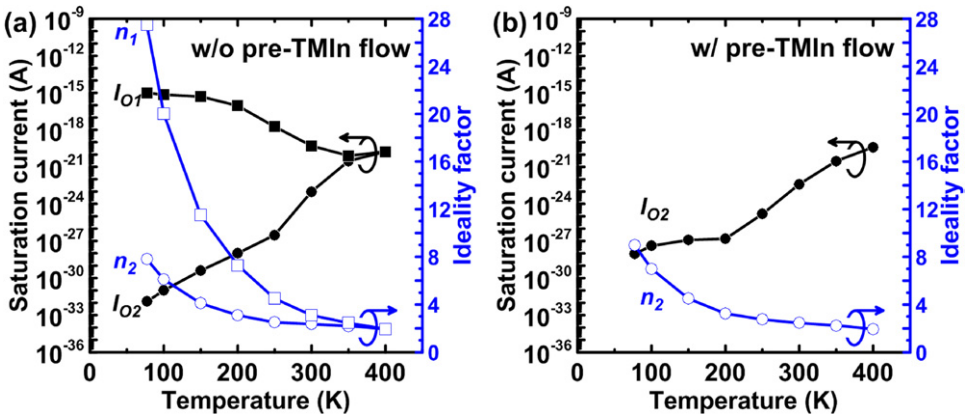

Figure 5. I_{O1}, I_{O2}, n_1 and n_2 versus temperature for LED samples (a) without and (b) with pre-TMIn flow treatment.

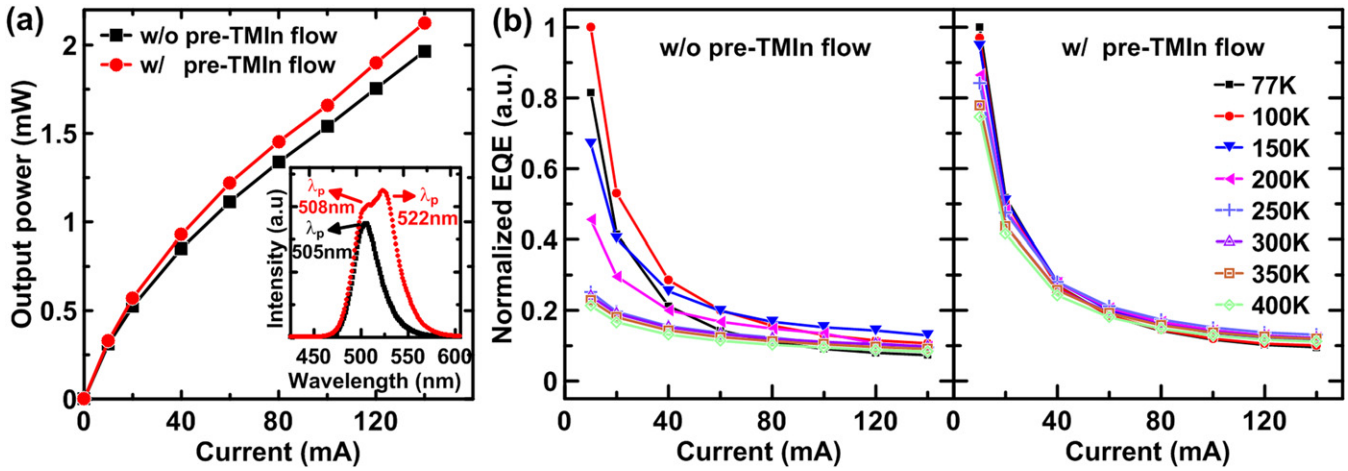

Figure 6. (a) Light output power versus injected current for both LED samples at $T = 300$ K. Inset: EL spectra with peak wavelengths. (b) EQE versus injected current for both LED samples from $T = 77$ to $T = 400$ K.

insensitive to temperature and have similar values as previously mentioned. The fitted I_{O1} and I_{O2}, and measured n_1, and n_2 as functions of temperature for both LED samples without and with pre-TMIn flow treatment are plotted in figures 5(a) and (b), respectively. In figure 5(a), at low temperatures ($77\,\text{K} < T < 250\,\text{K}$), the saturation current of the defect-assisted leakage process (I_{O1}) is remarkably larger than that of the diffusion–recombination process (I_{O2}), suggesting that most of the injected carriers recombine initially at the deep-level traps that are associated with dislocation defects, without any diffusion–recombination process. However, the difference in magnitude of saturation current between the defect-assisted leakage and the diffusion–recombination processes becomes less significant as the temperature increases, indicating that the diffusion–recombination current eventually dominates the LED at high temperatures. Figure 5(a) also suggests that the saturation current is an important index of the domination of the recombination of injected carriers in an InGaN-based LED. Also, the ideality factor is strongly temperature-dependent for both the defect-assisted leakage (n_1) and the diffusion–recombination (n_2) processes. Both n_1 and n_2 decrease as the temperature is increased. At a given temperature, n_1 is generally larger than n_2, causing the defect-assisted leakage current to be lower than the diffusion–recombination current, although I_{O1} is significantly larger than I_{O2}. In stark contrast, as shown in figure 5(b), one major recombination process of injected carriers dominates the I–V curve of the LED with pre-TMIn flow treatment. The calculated values of saturation current (I_{O2}) and the ideality factor (n_2) of the LED with the pre-TMIn flow treatment are similar to those of the LED without the pre-TMIn flow treatment. Restated, this suggests that when pre-TMIn flow is supplied, the influence of threading defects on the injected carriers is significantly reduced, promoting the diffusion–recombination of injected carriers, as well as the overall emission efficiency of the LED.

Finally, the temperature dependence of EQE of the LED samples is considered. Figure 6(a) shows the output power as a function of injected current for both LED samples of interest at $T = 300$ K. Clearly, the output power of the sample that underwent the pre-TMIn flow treatment is higher than that of the control sample. On average, the output power is enhanced by 9.5%. The inset in figure 6(a) plots the EL spectra for both samples for injected current $I = 20$ mA. Significantly, a stronger EL intensity with an additional peak is obtained at a longer wavelength ($\lambda = 522$ nm) from the LED sample with the pre-TMIn flow treatment, and could be due to its localized higher indium content in the QW compared with the conventional sample. Figure 6(b) plots the EQE

as a function of injected current for both LED samples from $T = 77$ K to $T = 400$ K. The maximum EQE is normalized in figure 6(*b*). The maximum EQE of both LED samples is observed to decrease with increasing temperature. In addition, for the LED without the pre-TMIn flow treatment, its EQE drops rapidly at low temperatures and the efficiency-droop behaviour is mitigated as the temperature increases. The rapid efficiency droop at low temperatures could originate from the low mobility and non-uniform distribution of injected holes in the LED [18, 19]. Therefore, with the increase in injected current, holes are confined in the QWs closest to the p-side and electrons exhibit serious leakage into the p-type GaN, resulting in constrained recombination of injected carriers in this QW [20]. As a result, a severe efficiency-droop behaviour is observed in LEDs without the pre-TMIn flow treatment at low temperatures. In general, the temperature-dependent efficiency droop of the LED with the pre-TMIn flow treatment follows a similar behaviour, as shown in figure 6(*b*). However, the EQE values of the sample that underwent the pre-TMIn flow treatment declines slightly as the temperature increases, demonstrating that the characteristics of this sample are more thermally stable. Studies have suggested that the injected carriers in the localized high indium content regions function excellently as radiative recombination centres, effectively suppressing the overflow of injected carriers outside the MQWs at elevated temperatures. This fact indicates that the pre-TMIn treatment can substantially reduce the dependence of EQE on temperature. In addition, the energy band profile was altered due to the incorporation of localized high indium content in QWs, which may reduce the influence of the quantum-confined stark effect. As a result, the overlap of electron–hole wave functions was significantly enhanced, also alleviating the efficiency droop [21, 22].

4. Summary

In summary, a pre-TMIn flow treatment was incorporated into an InGaN-based green LED to minimize the temperature dependence of EQE and alleviate the efficiency droop. For the LED sample with the pre-TMIn flow treatment, the tunnelling of injected carriers associated with threading defects is significantly reduced, promoting the diffusion–recombination of injected carriers, as well as the overall emission efficiency of the LED. Moreover, the presented device exhibits less efficiency droop at all measured temperatures. We therefore conclude that the pre-TMIn flow treatment is a promising scheme for the improvement of output performance of InGaN-based green LEDs and bridging the 'green gap' in solid-state lighting.

Acknowledgments

The authors gratefully acknowledge the financial support from the National Science Council of Republic of China (ROC) in Taiwan under contract No NSC–98–2112–M–003–001–MY2.

References

[1] Narukawa Y, Sano M, Ichikawa M, Minato S, Sakamoto T, Yamada T and Mukai T 2007 *Japan. J. Appl. Phys.* **46** L963
[2] Krames M R, Shchekin O B, Mueller-Mach R, Mueller G O, Zhou L, Harbers G and Craford M G 2007 *J. Disp. Technol.* **3** 160
[3] Crawford M H 2009 *IEEE J. Sel. Top. Quantum Electron.* **15** 1028
[4] Mukai T, Yamada M and Nakamura S 1999 *Japan. J. Appl. Phys.* **38** 3976–81
[5] Lee Y J, Chen C H and Lee C J 2010 *IEEE Photon. Technol. Lett.* **22** 1506
[6] Chichibu S F *et al* 2006 *Nature Mater.* **5** 810
[7] Liu J P, Jin R Q, Zhu J J, Zhang J C, Wang J F, Wu M, Chen J, Wang Y T and Yang H 2004 *J. Cryst. Growth* **264** 53
[8] Leem S-J, Kim M H, Shin J, Choi Y and Jeong J 2001 *Japan. J. Appl. Phys.* **40** L371
[9] Kumar M S, Park J Y, Lee Y S, Chung S J, Hong C-H and Suh E-K 2008 *Japan. J. Appl. Phys.* **47** 839
[10] Chen J, Wang J F, Wang H, Zhu J J, Zhang S M, Zhao D G, Jiang D S, Yang H, Jahn U and Ploog K H 2006 *Semicond. Sci. Technol.* **21** 1229
[11] Li Y, Zhao W, Xia Y, Zhu M, Senawiratne J, Detchprohm T, Schubert E F and Wetzel C 2007 *Phys. Status Solidi* c **4** 2784
[12] Cao X A, LeBoeuf S F, Kim K H, Sandvik P M, Stokes E B, Ebong A, Walker D, Kretchmer J, Lin J Y and Jiang H X 2002 *Solid-State Electron.* **46** 2291
[13] Cao X A, Teetsov J M, D'Evelyn M P, Merfeld D W and Yan C H 2004 *Appl. Phys. Lett.* **85** 7
[14] Shah J M, Li Y L, Gessmann Th and Schubert E F 2003 *J. Appl. Phys.* **94** 2627
[15] Lee S W *et al* 2006 *Appl. Phys. Lett.* **89** 132117
[16] Yamaguchi S, Kariya M, Nitta S, Amano H and Akasaki I 2000 *Japan. J. Appl. Phys.* **39** 2385
[17] Zhu D, Xu J, Noemaun A N, Kim J K, Schubert E F, Crawford M H and Koleske D D 2009 *Appl. Phys. Lett.* **94** 081113
[18] Cao X A and LeBoeuf S F 2007 *IEEE Trans. Electron Devices* **54** 3414
[19] Wang C H, Chen J R, Chiu C H, Kuo H C, Lee Y L, Lu T C and Wang S C 2010 *IEEE Photon. Technol. Lett.* **22** 236–8
[20] Chang J Y, Tsai M C and Kuo Y K 2010 *Opt. Lett.* **35** 1368–70
[21] Park S-H, Ahn D and Kim J-W 2009 *Appl. Phys. Lett.* **94** 041109
[22] Zhao H, Liu G, Li X-H, Hiang G S, Poplawsky J D, Penn S T, Dierolf V and Tansu N 2009 *Appl. Phys. Lett.* **95** 061104